Terahertz transitions in carbon nanotubes and graphene nanoribbons

V. A. Saroka * R. R. Hartmann† M. E. Portnoi‡

Abstract — **Interband dipole transitions are calculated in quasi-metallic single-walled carbon nanotubes and armchair graphene nanoribbons. It is shown that the curvature effects for tubes and the edge effects for ribbons result not only in a small band gap opening, corresponding to THz frequencies, but also in a significant enhancement of the transition probability rate across the band gap. This makes these nanostructures perspective canditates for sources and detectors of THz radiation.**

1 INTRODUCTION

Creating reliable, portable, tunable sources and detectors of terahertz radiation is one of the most challenging tasks of contemporary applied physics. One of the recent trends in bridging the so-called THz gap is the use of carbon-based nanostructures [1]. A number of schemes have been proposed so far [2, 3, 4, 5, 6]. Several original schemes utilizing the unique electronic properties of carbon nanotubes (CNTs) and graphene for THz application were brought forward by our group [7, 8, 9, 10, 11]. These schemes include THz generation by hot electrons in quasi-metallic CNTs, frequency multiplication in chiral-nanotube-based superlattices controlled by a transverse electric field, tunable THz radiation detection and optically-pumped emission in metallic CNTs in a strong magnetic field and using graphene p-n junctions for sub-wavelength polarization-sensitive THz detection. In this work we investigate possibility of utilizing direct interband dipole transitions in narrow-gap CNTs and graphene nanoribbons for THz devices.

2 CARBON NANOTUBES

Carbon nanotubes are cylindrical structures made from a single sheet of graphene rolled along a particular direction specified by the chiral vector, which for a two dimensional hexagonal lattice is described by two indices: n and m. Within the frame of a simple tight-binding model CNTs can either be metallic or semiconducting. If $n - m = 3p$, where p is an integer, then the tube is predicted to be metallic and have a linear energy dispersion with the conduction and valence bands touch at the point called the Dirac point. For zigag CNTs, which obey the condition $n = 3p$, $m = 0$, the Dirac point is positioned in the center of the Brillouin zone (BZ).

However, this simple model does not take into account the effect of curvature, which plays an important role for small diameter tubes ($1 - 2$ nm). It is now well established that curvature effects encompass three main contributions: the C-C bond contraction, π-orbital tilting and π- and σ-orbitals mixing [12]. All three contributions can be treated within the tight-binding model if one introduces corrections to the hopping integrals. With the exception of armchair nanotubes, these corrections result in a small band gap opening at the Dirac point of metallic CNTs. This means that these nanotubes are in fact quasi-metallic and have band gaps up to 50 meV [13, 14]. These small band gaps do not have much of an affect on the nanotubes' transport properties at room temperature because real samples of CNTs are always spuriously doped by chemicals used in the sample's preparation. However, the situation changes drastically for the optical properties of quasi-metallic tubes. Neglecting the effect of curvature, the probability rate of interband transitions between the closest valence and conduction subbands has a linear dependence on the electron wavevector measured form the Dirac point. This means that in the vicinity of the Dirac point interband transitions are suppressed. In contrast, if curvature effects are taken into account, interband transitions within a narrow region around the Dirac point become strongly allowed. As one can see from Fig. 1, there is a profound peak at the Dirac point for the magnitude of the velocity operator matrix element (VME), $v_{cv,T}$, as a function of the electron quasi-wavevector k measured with respect to the Dirac point. Hereafter, we consider only transition polarized along the structure axis. The peak has a characteristic height, which is independent of the tube's chirality and equal to the Fermi velocity of electrons in graphene ($v_F \approx 10^6$ m/s). The shape of the peak is described by the Lorentzian-like term

*Institute for Nuclear Problems, Belarusian State University, Bobruiskaya 11, 220030 Minsk, Belarus, e-mail: 40.ovasil@gmail.com.

†Physics Department, De La Salle University, 2401 Taft Avenue, Manila, Philippines, e-mail: richard.hartmann@dlsu.edu.ph.

‡School of Physics, University of Exeter, Stocker Road, Exeter EX4 4QL, United Kingdom, e-mail: m.e.portnoi@exeter.ac.uk.

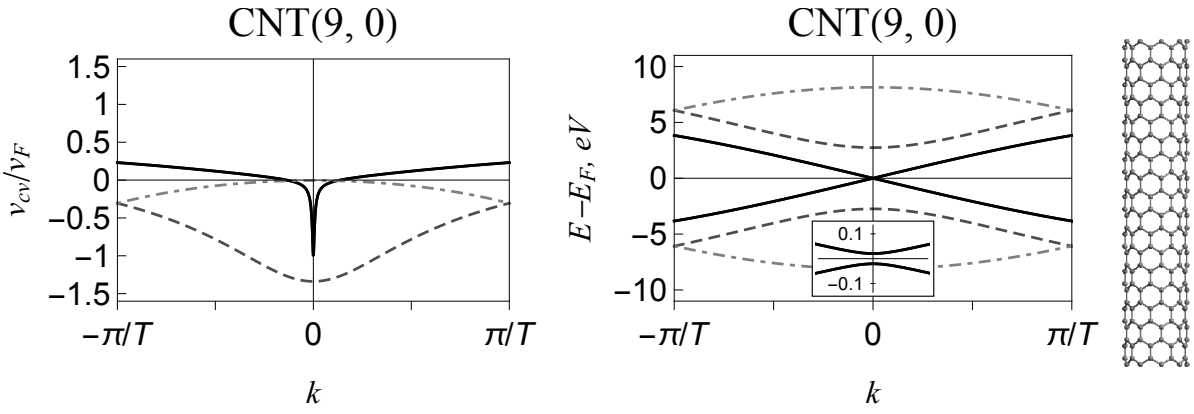

Figure 1: (Left) Velocity operator matrix elements in the BZ of a zigzag CNT for transitions between the closest valence and conduction subbands (thick, black), the lowest and highest subbands (dashed dotted, light gray), and the subbands, for which $|v_{cv}|$ attains the maximum possible value (dashed, gray), normalized by the Fermi velocity in graphene. (Right) The corresponding band and atomic structures. Inset zooms the region in the vicinity of the Dirac point, where $k = 0$.

in the expression:

$$v_{cv,T}(k) = v_F \left(\frac{a_0 \cos(3\theta)}{4} k - \frac{\Delta k}{\sqrt{\Delta k^2 + k^2}} \right) , \quad (1)$$

where $\Delta k = E_g/(2\hbar v_F)$, with E_g being the band gap, $a_0 = 0.142$ nm is the distance between the nearest carbon atoms and θ is the chiral angle. The chiral angle $\theta = 0$ and $\pi/6$ for zigzag and armchair tubes, respectively.

3 GRAPHENE NANORIBBONS

Graphene nanoribbons (GNRs) represents another type of quasi-one-dimensional carbon nanostructures, which can be imagined as narrow stripes cut from a single layer graphene sheet. The highest symmetry nanoribbons can be classified into the two types – zigzag and armchair. Within each of these classes a ribbon is uniquely specified by the number of carbon atom pairs N, or equivalently by the number of "zigzag lines" for zigzag or "dimer lines" for armchair nanoribbons. The most simple tight-binding model shows that all zigzag ribbons (ZGNR) are metallic, whereas only armchair ribbons (AGNRs) with $N = 3p - 2$, where p is an integer, are gapless. The low-energy dispersion of electrons in metallic AGNRs is linear and similar to that of metallic CNTs, while electron dispersion of ZGNRs is dominated by edge states. However, in actuality, both types of the metallic ribbons are quasimetallic. The electron dispersion of ZGNR edge states is strongly modified by electron-electron interaction, whereas for AGNR the energy dispersion is influenced by the change of C-C bonds at the edge of the ribbon compared to bonds in the ribbon interior. In both cases the outcome is a small band gap opening of the order of 50 meV [15].

In what follows we consider only quasi-metallic AGNRs, for which the edge effects lead to more prominent interband transitions between the closest valence and conduction subbands than for ZGNRs [16](triangular bilayer graphene clusters with zigzag edges also have weak interband transitions between the edge states [17]). The band structure of AGNRs can be obtained from that of graphene by a technique similar to that used for dealing with CNTs. In fact, there is an equivalence between the electronic properties of AGNR(N) to those of the zigzag CNT($N + 1, 0$) [18]. We show that this equivalence extends to optical transitions selection rules. The aforementioned edge effect in armchair ribbons can be again incorporated into the tight-binding model as small corrections to the hopping integrals [19]. Our calculations, presented in Fig. 2, show that the edge effect for quasi-metallic armchair GNRs results in a peak similar to that in Fig. 1. The peak has the same characteristic height and its shape can be well approximated by the second term of the equation (1).

4 DISCUSSION AND CONCLUSIONS

The main conclusion of the reported work is that there is a direct correspondence between single-walled zigzag CNTs and armchair GNRs. Curvature effects in quasi-metallic single-walled CNTs and edge effects in gapless armchair graphene nanoribbons not only open band gaps, which are typically in the THz range, but also result in a drastic enhancement of the probability of optical

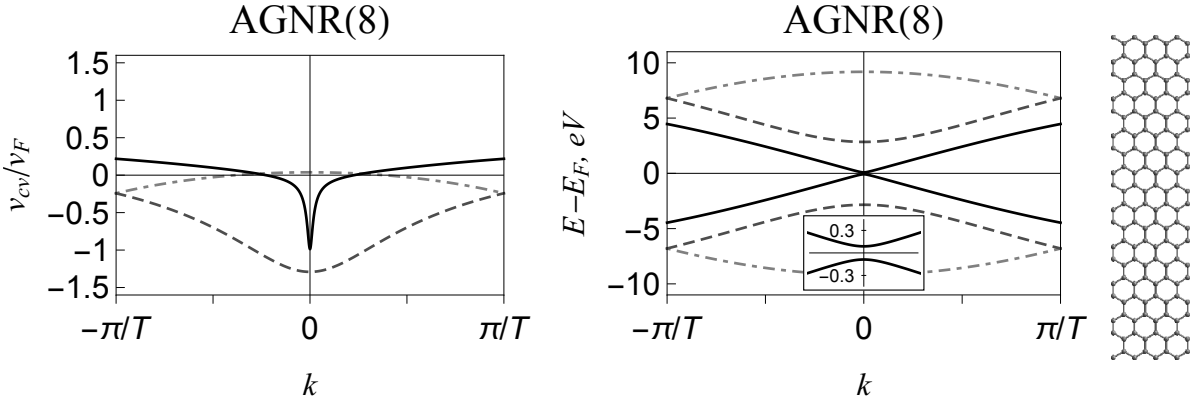

Figure 2: (Left) Velocity operator matrix elements in the BZ of an AGNR for transitions between the closest valence and conduction subbands (thick, black), the lowest and highest subbands (dashed dotted, light gray), and the subbands, for which $|v_{cv}|$ attains the maximum possible value (dashed, gray), normalized by the Fermi velocity in graphene. (Right) The corresponding band and atomic structures. Inset zooms the region in the vicinity of the Dirac point, where $k = 0$.

transitions across these gaps. The matrix element of the velocity operator for these transitions has a universal value, which is equal to the graphene Fermi velocity v_{F} when the photon energy coincides with the band gap E_{g}. Upon increasing the excitation energy, the absolute value of the transition matrix element first rapidly decreases, and thereafter it starts to increase proportionally to the photon frequency. Notably, the sharp transition peak near the band edge of quasi-metallic CNTs has been overlooked in the extensive literature on optical transitions in single-walled CNTs [20] and graphene nanoribbons [21, 22, 23, 24].

The described sharp photon-energy dependence of the transition matrix element together with the van Hove singularity at the band gap edge of the considered quasi-one-dimensional systems make them promising candidates for active elements in coherent THz radiation emitters. Such devices can be designed to be tunable by external fields. Magnetic field applied along the nanotube axis [9, 10] and electric field applied in to the ribbon in the in-plane geometry [25, 26] can provide an additional control of the frequency of the emitted radiation.

The effect of Pauli blocking of low-energy interband transitions caused by residual doping can be suppressed by creating a population inversion using high-frequency (optical) excitation. Excitonic effects, which are known to dominate the optical properties of semiconductor CNTs [27, 28] and GNRs [29], are of less importance in narrow-gap CNTs and ANGRs where the exciton binding energy is proportional to the bandgap [30] and dark excitonic states become irrelevant.

The effect similar to the edge effect in ribbons should also take place in a chemically functionalized graphene sheet with hydrogen, oxygen or fluorine adatoms adsorbed on its surface and leaving stripes of pure graphene intact. The electronic properties of thus produced graphene stripes have been predicted to be similar to those of GNRs [31]. The edge-like effects in the stripes arise from distortions caused by sp^3 hybridization of carbon atoms, which form chemical bonds with adatoms. The low-energy electronic properties are still determined by π-orbitals; therefore, the theoretical treatment of optical properties should be essentially the same as for nanoribbons. An additional tunability of the absorption frequencies of different stripes can be achieved by stretching the whole graphene sheet [32].

Finally, it is worth pointing out that armchair graphene nanoribbons of metallic family considered in this paper have been recently synthesised with atomically smooth edges by self-assembling of molecular precursors [33]. This advance in the ribbon synthesis should result in an increase of quality of ribbon samples and facilitate the experimental detection of the reported here THz transitions.

Acknowledgments

This work was supported by the EU FP7 ITN NOTEDEV (Grant No. FP7-607521); FP7 IRSES projects QOCaN (Grant No. FP7-316432), INTERNOM (Grant No. FP7-612624), CANTOR (Grant No. FP7-612285), H2020 RISE project CoExAN (Grant No. H2020-644076) and the British Council.

References

[1] R. R. Hartmann, J. Kono, and M. E. Portnoi, Nanotechnology **25**, 322001 (2014).

[2] K. Batrakov, S. Maksimenko, P. Kuzhir, and C. Thomsen, Phys. Rev. B, **79**, 125408 (2009).

[3] K. G. Batrakov, V. A. Saroka, S. A. Maksimenko, and C. Thomsen, J. Nanophoton. **6**, 061719 (2012).

[4] V. Ryzhii, M. Ryzhii, A. S. Satou, T. Otsuji, A. A. Dubinov, and V. Y. Aleshkin, J. Appl. Phys. **106**, 084507 (2009).

[5] V. Ryzhii, A. A. Dubinov, V. Y. Aleshkin, M. Ryzhii, and T. Otsuji, Appl. Phys. Lett. **103**, 163507 (2013).

[6] D. Svintsov, V. Ryzhii, A. Satou, T. Otsuji, and V. Vyurkov, Opt. Expr. **22**, 19873 (2014).

[7] O. V. Kibis, D. G. W. Parfitt, and M. E. Portnoi, Phys. Rev. B **71**, 035411 (2005).

[8] O. V. Kibis, M. Rosenau da Costa, and M. E. Portnoi, Nano Lett. **7**, 3414 (2007).

[9] M. E. Portnoi, O. V. Kibis, and M. Rosenau da Costa, Superlattices Microstruct **43**, 399 (2008).

[10] M. E. Portnoi, M. Rosenau da Costa, O. V. Kibis, and I. A. Shelykh, Int. J. Mod. Phys. B **23**, 2846 (2009).

[11] M. Rosenau da Costa, O. V. Kibis, and M. E. Portnoi , Microelectronics J. **40**, 776 (2009).

[12] J. C. Charlier and S. Roche, Rev. Mod. Phys. **79**, 677 (2007).

[13] M. Ouyang, J. L. Huang, C. L. Cheung, and C. M. Lieber, Science **292**, 702 (2001).

[14] Y. Matsuda, J. Tahir-Kheli, and W. A. Goddard, J. Phys. Chem. Lett. **1**, 2946 (2010).

[15] Y.-W. Son, M. L. Cohen, and S. G. Louie, Phys. Rev. Lett. **97**, 216803 (2006).

[16] V. A. Saroka, M. V. Shuba, and M. E. Portnoi, Phys. Rev. B **95**, 155438 (2017).

[17] H. Abdelsalam, M. H. Talaat, I. Lukyanchuk, M. E. Portnoi, and V. A. Saroka, J. Appl. Phys. **120**, 014304 (2016).

[18] C. T. White, J. Li, D. Gunlycke, and J. W. Mintmire, Nano Lett. **7**, 825 (2007).

[19] H. Zheng, Z. Wang, T. Luo, Q. Shi, and J. Chen, Phys. Rev. B **75**, 165414 (2007).

[20] S. Reich, C. Thomsen, and J. Maultzsch, Carbon Nanotubes, (WILEY-VCH Verlag GmbH and Co. KGaA, Weinheim, 2004) p. 215.

[21] M. F. Lin, and F. Shyu, J. Phys. Soc. Jap. **69**, 3529 (2000).

[22] H. Hsu, and L. Reichl, Phys. Rev. B **76**, 045418 (2007).

[23] H. Chung, M. Lee, C. Chang, and M. Lin, Opt. Expr. **19**, 197 (2011).

[24] K. Sasaki, K. Kato, Y. Tokura, K. Oguri, and T. Sogawa, Phys. Rev. B **84**, 085458 (2011).

[25] C. P. Chang, Y. C. Huang, C. L. Lu, J. H. Ho, T. S. Li, and M. F. Lin, Carbon **44**, 508 (2006).

[26] V. A. Saroka, K. G. Batrakov, V. A. Demin, and L. A. Chernozatonskii, J. Phys.: Condens. Matter **27**, 145305 (2015).

[27] J. Shaver and J. Kono, Laser and Photon. Rev. **1**, 260 (2007).

[28] J. Shaver, J. Kono, O. Portugall, V. Krstić, G. L. J. A. Rikken, Y. Miyauchi, S. Maruyama and V. Perebeinos, Nano Lett. **7**, 1851 (2007).

[29] R. Denk, M. Hohage, P. Zeppenfeld, J. Cai, C. A. Pignedoli, H. Söde, R. Fasel, X. Feng, K. Müllen, S. Wang, D. Prezzi, A. Ferretti, A. Ruini, E. Molinari, and P. Ruffieux, Nat. Communications **5**, 4253 (2014).

[30] R. R. Hartmann, I. A. Shelykh, and M. E. Portnoi, Phys. Rev. B **84**, 035437 (2011).

[31] L. A. Chernozatonskii, P. B. Sorokin, and J. W. Brüning, Appl. Phys. Lett. **91**, 183103 (2007).

[32] L. A. Chernozatonskii and P. B. Sorokin, J. Phys. Chem. C **114**, 3225 (2010).

[33] H. Zhang, H. Lin, K. Sun, L. Chen, Y. Zagranyarski, N. Aghdassi, S. Duhm, Q. Li, D. Zhong, Y. Li, K. Müllen, H. Fuchs, and L. Chi, J. Am. Chem. Soc. **137**, 4022 (2015).